

Supplementary Information for

**Comparison of Molecular Conductance between Planar and Twisted 4-Phenylpyridines
by Means of Two-Dimensional Phase Separation of Tetraphenylporphyrin Templates at
a Liquid–HOPG Interface**

Takeshi Sakano, Kenji Higashiguchi, and Kenji Matsuda*

*Department of Synthetic Chemistry and Biological Chemistry, Graduate School of
Engineering, Kyoto University, Katsura, Nishikyo-ku, Kyoto 615-8510, Japan*

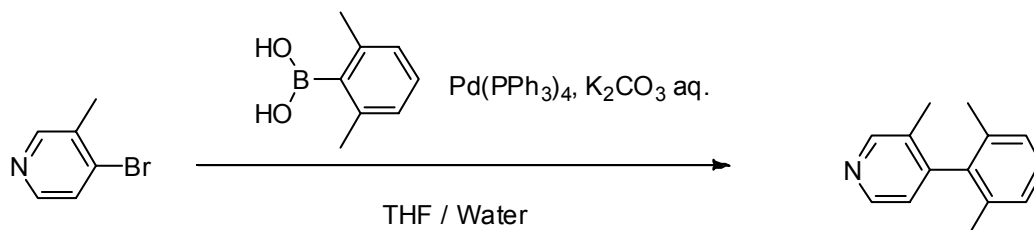
E-mail: kmatsuda@sbchem.kyoto-u.ac.jp

1. Experimental Details

Syntheses of the materials.

General. ^1H NMR spectra were recorded on a JEOL JMN-A500 instrument. Mass spectra were obtained by Bruker autoflex III MALDI-TOF mass spectrometer and Thermo Scientific Exactive mass spectrometer. All reactions were monitored by thin-layer chromatography carried out on 0.2 mm Merck silica gel plates (60F-254). Column chromatography was performed on silica gel (Nakarai, 70-230 mesh).

4-(2,6-Dimethylphenyl)-3-methylpyridine (2).



Tetrakis(triphenylphosphine)Palladium(0) (58 mg, 50 μmol), 2,6-dimethylphenylboronic acid (150 mg, 1.00 mmol), 4-bromo-3-methylpyridine^{S1} (172 mg, 1.00 mmol), and 20 wt% K_2CO_3 aqueous solution (4 mL) were mixed in THF (10 mL). The mixture was refluxed overnight. After cooled to room temperature, the mixture was extracted by diethyl ether. The organic layer was washed with brine, dried with Na_2SO_4 , and concentrated *in vacuo* after filtration. Purification by column chromatography (silica, chloroform) and GPC (chloroform) gave 4-(2,6-dimethylphenyl)-3-methylpyridine as a colorless oil (103 mg, 523 μmol , 52%). ESI HRMS (m/z) [$\text{M}+\text{H}$]⁺ calcd for $\text{C}_{14}\text{H}_{16}\text{N}$: 198.1277; found: 198.1277. ^1H NMR (CDCl_3 , 500 MHz, TMS) δ 1.94 (s, 6H), 1.98 (s, 3H), 6.99 (d, $J = 5$ Hz, 1H), 7.12–7.13 (m, 2H), 7.19–7.21 (m, 1H), 8.50 (d, $J = 5$ Hz, 1H), 8.55 (s, 1H).

21,23-Dihydro-5,10,15,20-tetrakis(4-hexadecyloxyphenyl)porphyrin ($\text{C}_{16}\text{-2H}$).^{S2}

MALDI TOF-HRMS (m/z) [$\text{M}+\text{H}$]⁺ calcd for $\text{C}_{108}\text{H}_{158}\text{N}_4\text{O}_4$: 1576.2356; found: 1576.2367. ^1H NMR (CDCl_3 , 500 MHz, TMS) δ 1.94 (s, 6H), 1.98 (s, 3H), 6.99 (d, $J = 5$ Hz, 1H), 7.12–7.13 (m, 2H), 7.19–7.21 (m, 1H), 8.50 (d, $J = 5$ Hz, 1H), 8.55 (s, 1H).

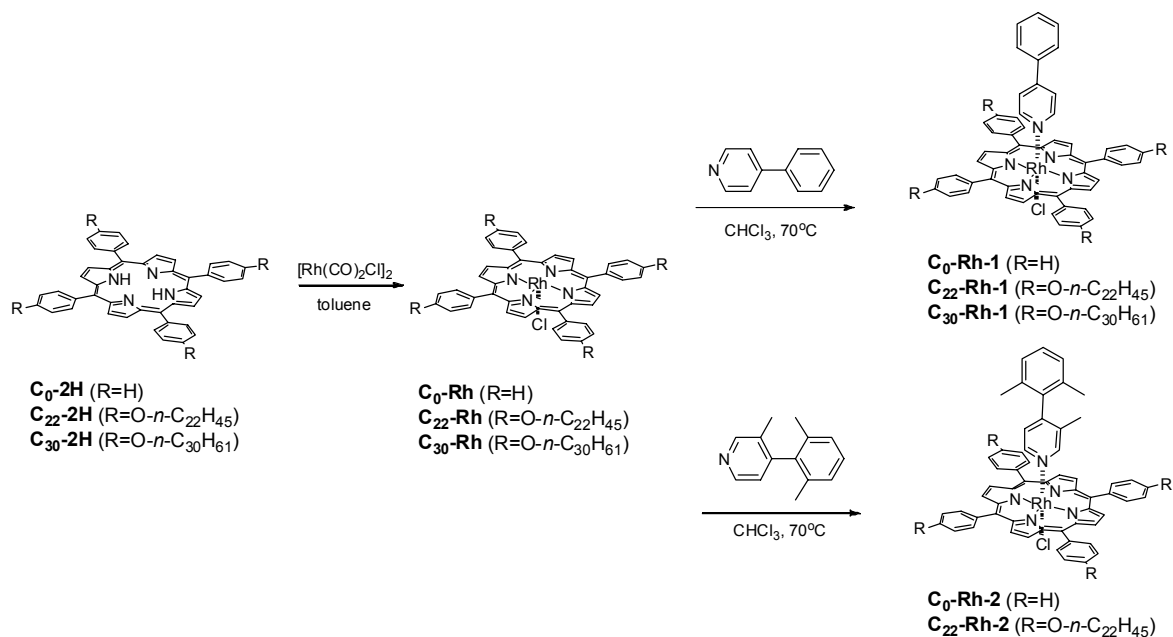
21,23-Dihydro-5,10,15,20-tetrakis(4-docosyloxyphenyl)porphyrin ($\text{C}_{22}\text{-2H}$).^{S3}

MALDI TOF-HRMS (m/z) [$\text{M}+\text{H}$]⁺ calcd for $\text{C}_{132}\text{H}_{207}\text{N}_4\text{O}_4$: 1912.6112; found: 1912.6080. ^1H NMR (CD_2Cl_2 , 500 MHz, TMS) δ -2.81 (s, 2H), 0.87 (s, 12H), 1.25–1.64 (m, 152H), 1.98 (quint, $J = 8$ Hz, 8H), 4.26 (t, $J = 7$ Hz, 8H), 7.29 (d, $J = 9$ Hz, 8H), 8.11 (d, $J = 9$ Hz, 8H), 8.89 (s, 8H).

21,23-Dihydro-5,10,15,20-tetrakis(4-triacontyloxyphenyl)porphyrin (**C₃₀-2H**).^{S4}

MALDI TOF-HRMS (m/z) [M]⁺ calcd for C₁₆₄H₂₇₀N₄O₄: 2360.1042; found: 2360.1066. ¹H NMR (CDCl₃, 500 MHz, TMS) δ -2.75 (s, 2H), 0.87 (t, J = 7 Hz, 12H), 1.20-1.41 (m, 208H), 1.48 (quint, J = 7 Hz, 8H), 1.63 (quint, J = 7 Hz, 8H), 1.98 (quint, J = 7 Hz, 8H), 4.35 (t, J = 7 Hz, 8H), 7.26 (d, J = 9 Hz, 8H), 8.10 (d, J = 9 Hz, 8H), 8.86 (s, 8H).

General procedure for the syntheses of phenylpyridine-coordinated TPP rhodium chlorides.^{S4}



1-Coordinated 5,10,15,20-tetrakisphenylporphyrin rhodium chloride (**C₀-Rh-1**).

Tetracarbonyl-di- μ -chlororhodium(I) (32.1 mg, 82.6 μ mol) and 5,10,15,20-tetraphenylporphyrin (50.0 mg, 81.3 μ mol) were dissolved in toluene. The mixture was refluxed overnight. The solvent was evaporated, and the residue was purified by column chromatography (chloroform). Red powder of TPP rhodium chloride (**C₀-Rh**) was obtained (33.9 mg, 45.1 μ mol). A part of **C₀-Rh** (7.7 mg, 10.25 μ mol) was added to a solution of 4-phenylpyridine (1.7 mg, 11.0 μ mol) in CHCl₃ (2 mL). The mixture was stirred for 1 h at 70 °C, and the solvent was evaporated *in vacuo*. Purification by column chromatography (silica, chloroform), GPC (chloroform) and HPLC (dichloromethane) gave **C₀-Rh-1** (2.3 mg, 2.54 μ mol, 25%) as red powder. ESI-HRMS (m/z) [$M+Na$]⁺ calcd for C₅₅H₃₇N₅ClRhNa: 928.1685; found: 928.1693. ¹H NMR (CDCl₃, 500 MHz, TMS) δ 1.01 (d, J = 6 Hz, 2H), 5.28 (d, J = 6 Hz, 2H), 6.53 (d, J = 8 Hz, 2H), 6.97 (t, J = 8 Hz, 2H), 7.05–7.06 (m, 1H), 7.69–7.77 (m, 12H), 8.12 (d, J = 8 Hz, 4H), 8.33–8.35 (m, 4H), 8.90 (s, 8H).

2-Coordinated 5,10,15,20-tetrakisphenylporphyrin rhodium chloride (C₀-Rh-2).

Yield: 19%, red powder. ESI-HRMS (*m/z*) [M+Na]⁺ calcd for C₅₈H₄₃N₅ClRhNa: 970.2154; found: 970.2184. ¹H NMR (CDCl₃, 500 MHz, TMS) δ 0.43 (s, 3H), 0.76 (s, 1H), 0.82 (s, 6H), 0.86 (d, *J* = 6 Hz, 1H), 4.72 (d, *J* = 6 Hz, 1H), 6.61 (d, *J* = 8 Hz, 2H), 6.81 (t, *J* = 8 Hz, 1H), 7.68–7.70 (m, 4H), 7.75–7.77 (m, 8H), 8.03 (d, *J* = 8 Hz, 4H), 8.37–8.38 (m, 4H), 8.89 (s, 8H).

1-Coordinated 5,10,15,20-tetrakis(4-docosyloxyphenyl)porphyrin rhodium chloride (C₂₂-Rh-1).

Yield: 21%, red powder. MALDI TOF-MS (*m/z*) [M-C₁₁H₉N]⁺ calcd for C₁₃₂H₂₀₄N₄O₄ClRh: 2047.462; found: 2047.521. ¹H NMR (CDCl₃, 500 MHz, TMS) δ 0.84 (d, *J* = 6 Hz, 2H), 0.88 (t, *J* = 7 Hz, 12H), 0.98 (d, *J* = 6 Hz, 2H), 1.25–1.48 (m, 144H), 1.62 (quint, 7 Hz, 8H), 1.98 (quint, 7 Hz, 8H), 4.24 (t, *J* = 7 Hz, 8H), 5.24 (d, *J* = 6 Hz, 2H), 6.51 (d, *J* = 8 Hz, 2H), 6.96 (t, *J* = 8 Hz, 2H), 7.05 (t, *J* = 8 Hz, 1H), 7.22 (dd, *J*₁ = 8 Hz, *J*₂ = 2 Hz, 4H), 7.28–7.29 (m, 4H), 8.02 (dd, *J*₁ = 8 Hz, *J*₂ = 2 Hz, 4H), 8.22 (dd, *J*₁ = 8 Hz, *J*₂ = 2 Hz, 4H), 8.92 (s, 8H).

2-Coordinated 5,10,15,20-tetrakis(4-docosyloxyphenyl)porphyrin rhodium chloride (C₂₂-Rh-2).

Yield: 29%, red powder. MALDI TOF-MS (*m/z*) [M-C₁₄H₁₅N]⁺ calcd for C₁₃₂H₂₀₄N₄O₄ClRh: 2047.462; found: 2047.532. ¹H NMR (CDCl₃, 500 MHz, TMS) δ 0.40 (s, 3H), 0.73 (s, 1H), 0.80 (s, 6H), 0.84 (d, *J* = 6 Hz, 1H), 0.88 (t, *J* = 7 Hz, 12H), 1.25–1.48 (m, 144H), 1.62 (quint, *J* = 7 Hz, 8H), 1.98 (quint, *J* = 7 Hz, 8H), 4.24 (t, *J* = 7 Hz, 8H), 4.68 (d, *J* = 6 Hz, 1H), 6.59 (d, *J* = 8 Hz, 2H), 6.79 (t, *J* = 8 Hz, 1H), 7.21 (dd, *J*₁ = 8 Hz, *J*₂ = 2 Hz, 4H), 7.28 (dd, *J*₁ = 8 Hz, *J*₂ = 2 Hz, 4H), 7.92 (dd, *J*₁ = 8 Hz, *J*₂ = 2 Hz, 4H), 8.25 (dd, *J*₁ = 8 Hz, *J*₂ = 2 Hz, 4H), 8.92 (s, 8H).

1-Coordinated 5,10,15,20-tetrakis(4-triacontyloxyphenyl)porphyrin rhodium chloride (C₃₀-Rh-1).

Yield: 33%, red powder. MALDI TOF-MS (*m/z*) [M-C₁₁H₉N+H]⁺ calcd for C₁₆₄H₂₆₉N₄O₄ClRh: 2496.971; found: 2496.729. ¹H NMR (CDCl₃, 500 MHz, TMS) δ 0.86 (t, 12H), 0.98 (d, *J* = 7 Hz, 2H), 1.25–1.48 (m, 208H), 1.62 (quint, *J* = 7 Hz, 8H), 1.98 (quint, *J* = 7 Hz, 8H), 4.24 (t, *J* = 7 Hz, 8H), 5.24 (d, *J* = 7 Hz, 2H), 6.51 (d, *J* = 8 Hz, 2H), 6.96 (t, *J* = 8 Hz, 2H), 7.05 (t, *J* = 8 Hz, 1H), 7.22–7.29 (m, 8H), 8.02 (dd, *J*₁ = 8 Hz, *J*₂ = 2 Hz, 4H), 8.02 (dd, *J*₁ = 8 Hz, *J*₂ = 2 Hz, 4H), 8.86 (s, 8H).

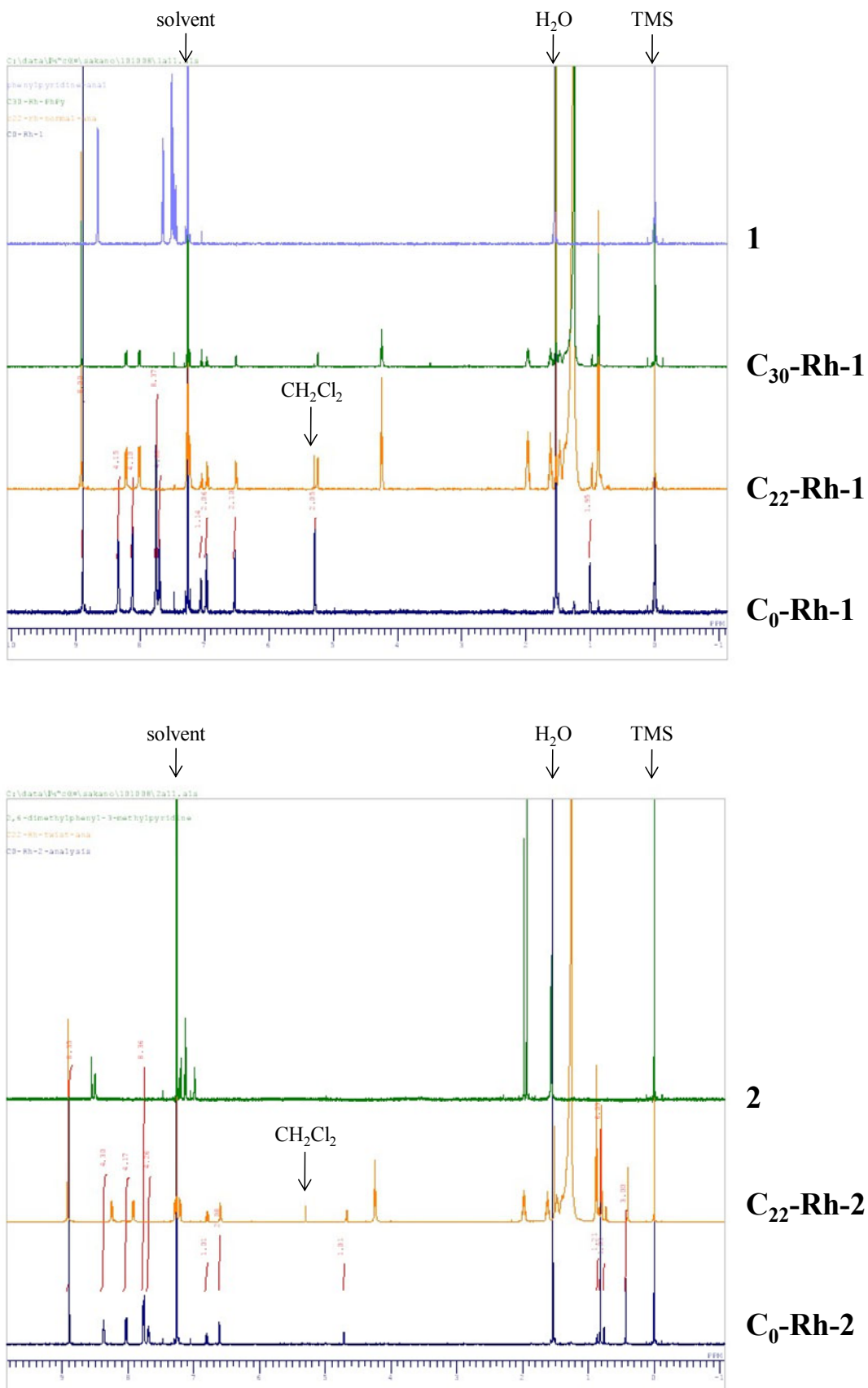


Figure S1. NMR charts of the synthesized compounds.

STM Measurements. All STM experiments were performed at room temperature and ambient conditions. The STM images were acquired with a Digital Instrument Multimode Nanoscope IIIa and obtained at liquid-solid interface. All STM images were acquired in the constant current mode. The STM tips were electrochemically etched in a CaCl_2/HCl aqueous solution from Pt/Ir (80/20, diameter 0.25 mm) wire. Highly oriented pyrolytic graphite purchased from the Veeco Metrology Group was used as a substrate. The calibration of the piezoelectric position was verified by atomic resolution imaging of graphite (x- and y-directions) and by the height of single steps on the graphite surface (z-direction). Concentrations of the solution used for STM measurements were checked by absorption spectroscopy ($\text{Abs}_{\text{solet}} = 0.03$ to 2.0, light path 4 mm).

X-ray Crystallography. **C₀-Rh-1** and **C₀-Rh-2** were recrystallized from acetone and methanol, respectively, to give red needles in both cases. X-ray crystallographic analysis was performed using a Bruker APEX II diffractometer (55 kV, 35 mA) with Mo $K\alpha$ radiation. The data were collected as a series of ω -scan frames. Data reduction was performed using SAINT software and the cell constants were calculated by the global refinement. Absorption correction was performed numerically based on the measured crystal shape. The structure was solved by direct methods using SHELXS and refined by full least-squares on F^2 using SHELXL.^{S5} The positions of all hydrogen atoms were calculated geometrically and refined by the riding model. CCDC 814313 and 814314 contain the supplementary crystallographic data for **C₀-Rh-1** and **C₀-Rh-2**, respectively.

Crystal data for **C₀-Rh-1**: $\text{C}_{61}\text{H}_{49}\text{N}_5\text{O}_2\text{ClRh}$, $FW = 1022.43$, monoclinic, Cc , $a = 17.5590(8)$ Å, $b = 15.5831(7)$ Å, $c = 18.4654(8)$ Å, $\beta = 105.247(1)^\circ$, $V = 4874.7(4)$ Å³, $Z = 4$, $R_1 [I > 2\sigma(I)] = 0.0373$, $wR_2 = 0.0846$. **C₀-Rh-2**: $\text{C}_{59}\text{H}_{47}\text{N}_5\text{OClRh}$, $FW = 980.3959$, monoclinic, Cc , $a = 17.7891(12)$ Å, $b = 13.8346(11)$ Å, $c = 20.6811(19)$ Å, $\beta = 111.2830(10)^\circ$, $V = 4742.6(6)$ Å³, $Z = 4$, $R_1 [I > 2\sigma(I)] = 0.0477$, $wR_2 = 0.1343$.

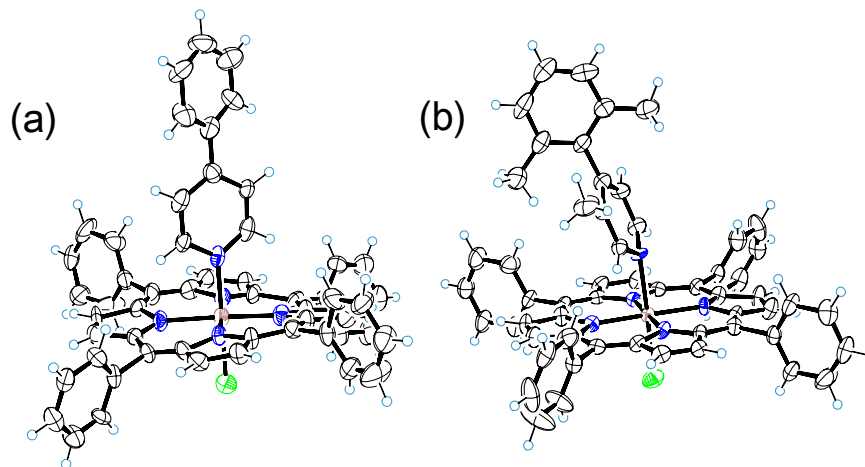


Figure S2. ORTEP drawings of the X-ray crystallographic structures of (a) **C₀-Rh-1** and (b) **C₀-Rh-2**. Solvents are omitted from the figures for clarity.

2. STM image of C₁₆-2H, C₂₂-2H, and C₃₀-2H

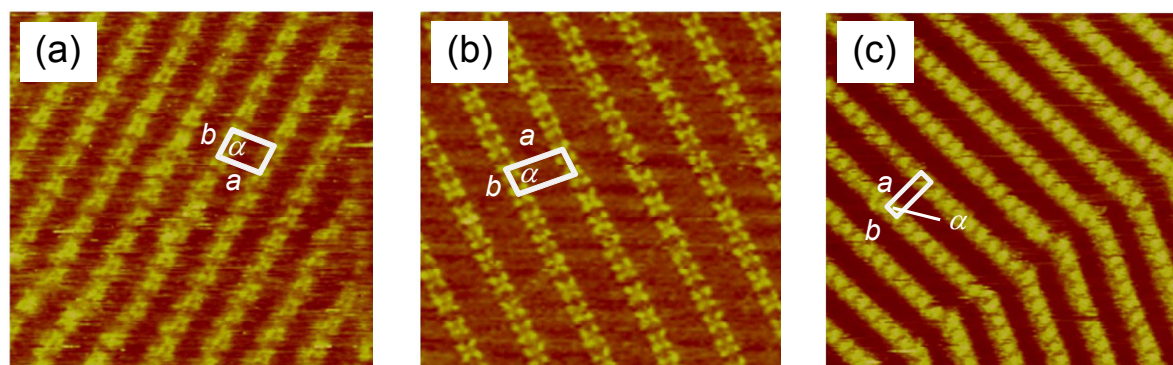


Figure S3. STM images at the liquid–HOPG interface in the constant current mode:

- (a) C₁₆-2H (1-phenyloctane, 25 × 25 nm², $I_{\text{set}} = 30$ pA, $V_{\text{bias}} = -1.0$ V);
(b) C₂₂-2H (1-phenyloctane, 25 × 25 nm², $I_{\text{set}} = 30$ pA, $V_{\text{bias}} = +1.0$ V);
(c) C₃₀-2H (1,2,4-trichlorobenzene, 40 × 40 nm², $I_{\text{set}} = 30$ pA, $V_{\text{bias}} = -1.0$ V).

3. Relationship between carbon atom number of side chain and lattice parameter *a*

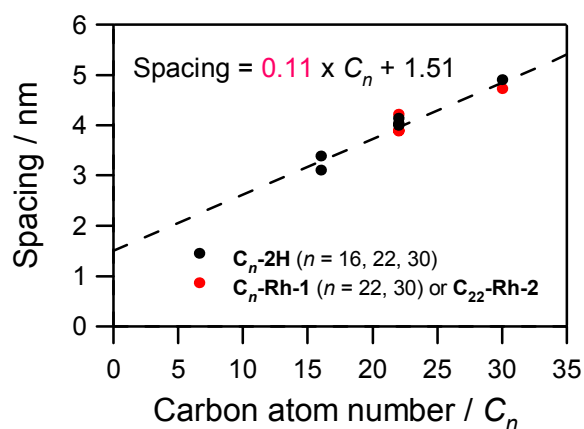


Figure S4. Relationship between the carbon atom number (C_n) of side chain and the lattice parameter a for TPPs C₁₆-2H, C₂₂-2H, C₃₀-2H, C₂₂-Rh-1, C₂₂-Rh-2, and C₃₀-Rh-1. Linear fitting of the plot gives the slope of 0.11 nm per carbon atom.

4. Lattice parameters of unit cell for TPPs

Table S1. Obtained lattice parameters of unit cell.

compound	solvent		<i>a</i> /nm	<i>b</i> /nm	α /°
C₁₆-2H (Fig. S3a)	phenyloctane		3.1	2.0	83
C₂₂-2H (Fig. S3b)	phenyloctane		4.1	1.9	84
C₃₀-2H (Fig. S3c)	1,2,4-trichlorobenzene		4.9	1.7	86
C₁₆-2H+C₂₂-2H (Fig. 3)	phenyloctane	smaller	3.4	1.8	89
		larger	4.0	1.6	88
C₂₂-Rh-1 (Fig. 2a)	ocatanoic acid		3.9	1.8	71
C₂₂-Rh-1+C₂₂-Rh-2 (Fig. 2b)	ocatanoic acid		4.2	2.3	82
C₃₀-Rh-1+C₂₂-Rh-2 (Fig. 4)	ocatanoic acid	smaller	3.9	1.7	85
		larger	4.7	1.7	83

References

- S1 A. C. Spivey, L. Shukla, J. F. Hayler, *Org. Lett.*, 2007, **9**, 891–894.
S2 J. H. van Esch, M. C. Feiters, A. M. Peters, R. J. M. Nolte, *J. Phys. Chem.*, 1994, **98**, 5541–5551.
S3 J. Otsuki, S. Kawaguchi, T. Yamakawa, M. Asakawa, K. Miyake, *Langmuir*, 2006, **22**, 5708–5715.
S4 T. Ikeda, M. Asakawa, M. Goto, K. Miyake, T. Ishida, T. Shimizu, *Langmuir*, 2004, **20**, 5454–5459.
S5 *APEX2 Software Package ver. 2.0*, Bruker AXS, Madison, WI 2005.